



**HAL**  
open science

# Role of the TiO octahedra on the ferroelectric and piezoelectric behaviour of the poled PbMgNbO-xPbTiO (PMN-PT) single crystal and textured ceramic

A. Slodczyk, Ph. Colomban, M. Pham-Thi

► **To cite this version:**

A. Slodczyk, Ph. Colomban, M. Pham-Thi. Role of the TiO octahedra on the ferroelectric and piezoelectric behaviour of the poled PbMgNbO-xPbTiO (PMN-PT) single crystal and textured ceramic. Journal of Physics and Chemistry of Solids, 2009, 69 (10), pp.2503. 10.1016/j.jpcs.2008.05.004 . hal-00581986

**HAL Id: hal-00581986**

**<https://hal.science/hal-00581986>**

Submitted on 1 Apr 2011

**HAL** is a multi-disciplinary open access archive for the deposit and dissemination of scientific research documents, whether they are published or not. The documents may come from teaching and research institutions in France or abroad, or from public or private research centers.

L'archive ouverte pluridisciplinaire **HAL**, est destinée au dépôt et à la diffusion de documents scientifiques de niveau recherche, publiés ou non, émanant des établissements d'enseignement et de recherche français ou étrangers, des laboratoires publics ou privés.

## Author's Accepted Manuscript

Role of the  $\text{TiO}_6$  octahedra on the ferroelectric and piezoelectric behaviour of the poled  $\text{PbMg}_{1/3}\text{Nb}_{2/3}\text{O}_3-x\text{PbTiO}_3$  (PMN-PT) single crystal and textured ceramic

A. Slodczyk, Ph. Colomban, M. Pham-Thi

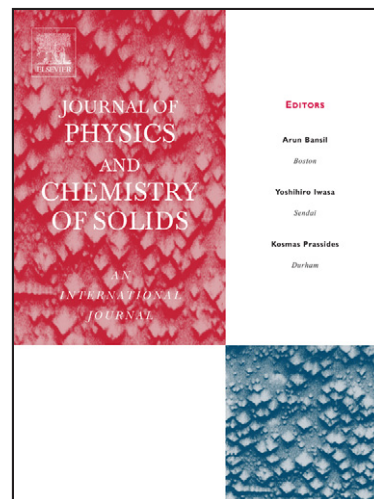
PII: S0022-3697(08)00172-8  
DOI: doi:10.1016/j.jpcs.2008.05.004  
Reference: PCS 5490

To appear in: *Journal of Physics and Chemistry of Solids*

Received date: 13 November 2007  
Revised date: 15 April 2008  
Accepted date: 7 May 2008

Cite this article as: A. Slodczyk, Ph. Colomban and M. Pham-Thi, Role of the  $\text{TiO}_6$  octahedra on the ferroelectric and piezoelectric behaviour of the poled  $\text{PbMg}_{1/3}\text{Nb}_{2/3}\text{O}_3-x\text{PbTiO}_3$  (PMN-PT) single crystal and textured ceramic, *Journal of Physics and Chemistry of Solids*, doi:10.1016/j.jpcs.2008.05.004

This is a PDF file of an unedited manuscript that has been accepted for publication. As a service to our customers we are providing this early version of the manuscript. The manuscript will undergo copyediting, typesetting, and review of the resulting galley proof before it is published in its final citable form. Please note that during the production process errors may be discovered which could affect the content, and all legal disclaimers that apply to the journal pertain.



[www.elsevier.com/locate/jpcs](http://www.elsevier.com/locate/jpcs)

**Role of the TiO<sub>6</sub> octahedra on the ferroelectric and piezoelectric behaviour of the poled PbMg<sub>1/3</sub>Nb<sub>2/3</sub>O<sub>3</sub>-xPbTiO<sub>3</sub> (PMN-PT) single crystal and textured ceramic**

**A. Slodczyk<sup>1</sup>, Ph. Colomban<sup>1\*</sup> and M. Pham-Thi<sup>2</sup>**

<sup>1</sup> *Laboratoire de Dynamique, Interactions et Réactivité (LADIR), UMR 7075*

*CNRS*

*Université Pierre et Marie Curie (UPMC Univ Paris 06)*

*2 rue Dunant, 94320 Thiais, France*

<sup>2</sup> *Thales Research & Technology France,*

*91404 Orsay, France*

\*corresponding author

**Abstract.**

Field cooling (FC) poled/unpoled PMN-29%PT single crystal and room temperature (RT) poled/unpoled PMN-34.5%PT textured ceramic were investigated between ~0° and 300°C by thermal expansion, dielectric and Raman spectroscopy. New phase transitions are evidenced at 40°C, 91°C and 180°C in the case of FC PMN-29%PT as well as at 70°C and 200°C for RT PMN-34.5%PT and their order is discussed. The physical properties of the textured ceramics are rather similar to those ones observed for the single crystals what makes them the low cost alternative for a wide application. However, the temperatures and character of the phase transitions are strongly dependent on the kind of the poling conditions. Temperature dependences of the Raman line parameters show that the NbO<sub>6</sub> octahedra remain stable during temperature increasing while TiO<sub>6</sub> ones evolve quasi continuously. The step transitions of the Pb<sup>2+</sup> ion

sublattice are evidenced. This suggests that the  $\text{TiO}_6$  and  $\text{Pb}^{2+}$  sublattices are especially coupled. The role of the  $\text{TiO}_6$  clusters on the structural phase transitions and the dielectric properties of the PMN-PT system is discussed. The presence of the Raman modes above the maximum of dielectric permittivity reveals that the local symmetry is lower than the cubic one ( $\text{Pm}3\text{m}$ ). The decrease of the Raman line intensities vs. temperature indicates precisely the continuous evolution of the local symmetry towards the cubic one. The temperature evolution of the Rayleigh wing parameters appears sensitive to the phase transitions presence.

**Keywords** C. Raman spectroscopy, D. dielectric properties, D. ferroelectricity, D. phase transitions, D. piezoelectricity, D. thermal expansion

**Corresponding author**

Philippe Colomban

[philippe.colomban@glvt-cnrs.fr](mailto:philippe.colomban@glvt-cnrs.fr)

tel: 0033 1 49781105

fax: 0033 149781118

**Introduction.**

Lead magnesium niobate–lead titanate solid solutions  $\text{PbMg}_{1/3}\text{Nb}_{2/3}\text{O}_3$ - $x\text{PbTiO}_3$ , i.e. PMN-PT, have been recently intensively studied due to their outstanding dielectric and electromechanical properties [1,2]. Extremely large values of the dielectric constant, giant piezoeffect, ultrahigh strain and electrostriction were reported for PMN-PT single crystals properly orientated and poled along non-polar direction. This is related to the fact that the crystal domains easily orient during poling so that the maximum response is obtained. Therefore, these solid solutions are very interesting from the application point view and provide the excellent opportunity for improvements in sonar applications, active damping, high strain actuators, medical ultrasonic imaging, etc. However, the methods of obtaining the large enough single crystals for such application are very expensive and complicated. Thus, the strongly oriented or textured ceramics made in the low-cost production are a very good alternative [3-8].

PMN-PT solid solutions exhibit a great variety of structural, vibrational and dielectric properties which are strongly dependent on the PT content. Different phase diagrams have been proposed [9-11] (see Figure 1). According to the common part of these zero-field phase diagrams the PMN-PT solid solutions with the PT content lower than 30% possess the typical relaxor behaviour characterized by the broad and strongly frequency dependent maximum of dielectric permittivity. With the temperature increasing they exhibit the rhombohedral ( $R3m$ )  $\rightarrow$  cubic ( $Pm3m$ ) structural phase transition. The materials with the PT content higher than 38% present the ferroelectric behaviour and on heating they undergo the tetragonal ( $P4mm$ )  $\rightarrow$  cubic ( $Pm3m$ ) structural phase transition. These two characteristic regions: relaxor and ferroelectric ones, are separated by the so-called morphotropic phase boundary (MPB). It must be stressed that the excellent electromechanical properties and the giant piezoeffect are

observed for the solid solutions with compositions belonging to the MPB. In general, these materials possess already ferroelectric behaviour and undergo the monoclinic (Pm)  $\rightarrow$  tetragonal (P4mm)  $\rightarrow$  cubic (Pm3m) structural phase transitions [11,12]. However, many authors [11, 13-17] suggested that the symmetry observed in the vicinity of the MPB is more complex. Namely, the monoclinic symmetry can coexist with a secondary minority phases: tetragonal or rhombohedral, and the presence of the orthorhombic phase was also postulated. The existence of additional weak phase transitions below room temperature which sequence strongly depends on the poling procedure was evidenced by the thermal expansion measurements [18]. These results reveal that the different symmetries observed in the vicinity of the MPB are energetically very close and thus the coexistence as well as the transitions between them are very probable [2,19]. Moreover, the sequence of structural phase transitions can be easily changed by the influence of the physical parameters such as pressure, electric field and the kind of polarization [18,20,21]. For example, it was demonstrated that the previously poled PMN-35%PT solid solutions adopt the monoclinic symmetry with the Cm space group at room temperature [22].

The polarization is one of the most important parameters determining the behaviour of the PMN-PT system and is considered to play the key role in the appearance of the giant piezoelectricity. According to the polarization rotation theory [2,19] the polarization vector characteristic for the solid solution from the MPB is not fixed in one crystallographic direction as in the case of the typical ferroelectrics but can continuously rotate in the planes (110) or (010). However, it should be underlined that despite the intensive studies the physical properties of the solid solutions from the MPB region and directly connected with them electromechanical ones are still not well understood.

The aim of our work is to investigate and compare the relation between the local structure and the kind of poling conditions: field cooling (FC) or room temperature (RT) poling, on the physical properties of the solid solutions from the vicinity of the MPB: PMN-29%PT single crystal and PMN-34.5% textured ceramic. Therefore, we have undertaken the comparison Raman scattering studies between the poled (FC or RT) and unpoled /depoled materials. Since the physics of relaxor ferroelectric solid solutions takes place mainly on the nanoscale, the Raman spectroscopy due to its sensitivity to the local symmetry is a very useful technique to investigate these compounds. In order to better understand and describe the Raman features they were compared with our own thermal expansion and dielectric results performed on the same samples. In this first paper we present the results obtained for the FC poled/ unpoled PMN-29%PT single crystal and RT poled/ unpoled PMN-34.5% textured ceramic. In the second paper the results performed on the same samples but opposite polarized, i.e. RT poled single crystal and FC textured ceramic will be presented.

## 2. Experimental procedure

The experiments were performed on the PMN-29%PT single crystal from APC (USA) and the PMN-34.5%PT textured ceramic (Lotgering factor = 0.9) prepared at R&T Thales. The details concerning the method of obtaining this ceramic are available in [3-5]. The PMN-29%PT was poled by the field cooling method, namely the electric field of strength 200V/mm was applied at 170°C and then the crystal was cooled in the presence of the electric field up to -20°C . The textured ceramic was poled in the room temperature by applying the electric field of the strength of 800V/mm. The unpoled state for both materials was obtained by the heating the samples till temperature two hundreds °C higher than the temperature of maximum of dielectric permittivity (~140°C

for single crystal and  $\sim 160^\circ\text{C}$  for textured ceramic) at least two times. At such high temperature the sample was kept  $\sim 10$  minutes.

The Raman spectra for both samples were collected in the macro configuration and backscattering geometry (spot  $\sim 300\mu\text{m}$ , laser power 30mW, resolution  $\sim 0.8\text{ cm}^{-1}$ ) using an XY spectrograph (Dilor, France) equipped with a double monochromator filter and a back illuminated, liquid nitrogen cooled CCD detector. The 514.5 nm and 632 nm  $\text{Ar}^+$  laser excitation lines were used. Raman spectra were collected in the low and middle frequency range ( $40\text{-}1200\text{cm}^{-1}$ ) from  $20^\circ\text{C}$  to  $240^\circ\text{C}$ , using the home made furnace. Measurements were taken every  $20^\circ\text{C}$  during 20 minutes. Additionally, in each value of temperature the Rayleigh line was recorded. The heating rate was  $0.5^\circ/\text{min}$ . The intensities and widths of the Rayleigh wings were approximated using the triangle method. In order to determine the temperature dependences of the Raman line parameters: position, full width at half maximum (FWHM) and intensity, the spectra were decomposed using the Origin Peak Fitting software. Before the decomposition the Raman spectra were corrected by the Bose-Einstein population factor. During the fitting the linear baseline was used and a Gaussian shaped was assumed for all Raman lines.

The thermal expansion measurements were carried out using a Setaram (France) instrument (Setsys) equipped with the amorphous silica rod and support. A cryostat – furnace working in the temperature range from  $-200^\circ\text{C}$  to  $400^\circ\text{C}$  was used. The measurements were recording both in the heating and cooling cycles with the rates of  $5^\circ/\text{min}$ .

Dielectric measurements were performed at frequency of 1KHz. The heating cycle was recording for unpoled and freshly poled samples. The heating cycles were collected with the rate of  $\sim 1^\circ/\text{min}$ .

Note a small, i.e.  $\pm 5^\circ\text{C}$ , temperature difference possible between the techniques.

### 3. Results and Discussion

#### *Dielectric and thermal expansion studies*

Figure 2 presents the results of the thermal expansion and dielectric studies in the function of temperature for poled and unpoled: PMN-29%PT single crystal and PMN-34.5%PT textured ceramic. As it can be clearly seen these results point to the presence of complex sequence of the structural phase transitions. Note that the temperatures as well as the character of these phase transitions are different for poled and unpoled materials. It is noteworthy that the maximal values of the dielectric permittivity recorded for textured ceramics are very high, almost comparable with those ones recorded for single crystals. Moreover, the thermal expansion measurements shown in Figure 3 reveal the anisotropic character of the textured ceramic, namely the thermal expansion curves recorded along x, y, z directions of cut ceramic, close to [100], [010] and [001] crystallographic directions, are different. This clearly confirms the application potential of the textured ceramics in the place of single crystals.

As it can be seen in Figure 2 the FC poled PMN-29%PT single crystal exhibits two sharp maxima of dielectric permittivity of the ferroelectric character observed at 91°C and 134°C. Actually, near 91°C two maxima appear. The thermal expansion curve shows the anomalies near the similar values of temperatures. The dilatometry data point to the presence of two additional weak phase transitions near 40 and 200°C, already detected in a preliminary work[18]. These additional phase transitions correspond to the onset of the increase and then the decrease of the dielectric permittivity, respectively. In the case of unpoled PMN-29%PT two phase transitions are also detected by the dielectric permittivity at about 118°C and 140°C. However, in comparison with those ones observed for poled crystal they have rather relaxor character [23,24]. Namely, they are quite broad and the temperature of the maximum of dielectric permittivity is

frequency dependent. This shows that the ferroelectric state can be achieved only after the FC polarization. Note that similar results were detected for the PMN-26PT single crystal for which sharp ferroelectric peak was recorded when the sample was previously poled [25]. Two phase transitions recorded for the unpoled PMN-29%PT single crystal are also detected by the thermal expansion curve. The main phase transition observed near 140°C is marked very clearly whereas that one appearing at 114°C is very weak.

The temperature dependence of the dielectric permittivity recorded for the RT poled PMN-34.5%PT textured ceramic is rather similar to that observed for the FC poled PMN-29%PT but anomalies are more smoothed. The main maximum of the dielectric permittivity is observed at ~160°C. Note that very similar maximum of the dielectric permittivity detected exactly at the same temperature is present for unpoled PMN-34.5%PT textured ceramic. This shows that the character and temperature of the main maximum of dielectric permittivity seem to be independent of the poling conditions what proves that this solid solution possesses already the ferroelectric behaviour. Note that in the case of relaxors the kind of polarization change significantly the temperature and character of phase transitions whereas for the ferroelectrics the role of polarization seems to be less important. In the case of poled ceramic the additional very weak maximum of dielectric permittivity was detected near 70°C. The thermal expansion curve recorded for RT poled sample shows a bump near 160°C. Such continuous slope variations correspond very well to the step variations character recorded for the single crystal. The anisotropic character of the dilatometric data shown in Figure 3 confirms the similarity between the thermal expansion behaviour of the textured ceramic and the single crystal. For the unpoled ceramic the thermal expansion anomalies are very smooth even in the case of the main phase transition.

The thermal expansion data show clearly the presence of the temperature hysteresis in the case of PMN-29%PT in the vicinity of the main phase transition [18]. The temperature hysteresis is also observed in the dielectric measurements (see Figure 4). Note that this thermal hysteresis seems to be less important in the case of the textured ceramic. Since the appearing of the hysteresis is directly connected with the phase transition character the complementary dielectric and dilatometry results suggest that most of the observed phase transitions are of the first order.

The main phase transition observed at 134°C and at 140°C for the FC poled and unpoled single crystals, respectively can be attributed (according to the diffraction data [11,13,17]) to the transition from the rhombohedral symmetry to the cubic paraelectric one. Similar, the main transitions detected near 160°C in the case of RT poled/unpoled texture ceramic might be assigned to the transition from the tetragonal symmetry to the cubic one. However, the origin of the additional phase transition detected at lower temperatures needs clarification. In the case of the PMN-29%PT the Noheda' phase diagram [11] does not show such phase transition. However, recently some articles appears in which additional phase transition was observed in the solid solutions with similar compositions: 27%PT and 29%PT [13,16,17] and interpreted as structural phase transitions from the monoclinic (Cm or Pm space group) to the rhombohedral symmetry. Moreover, even presence of structural phase transitions between two different monoclinic symmetry and/or the coexistence of the phases (two monoclinic or rhombohedral-monoclinic) were suggested [13,17]. For the PMN-34.5%PT solid solution the Noheda phase diagram [11] as well as different articles show the possibility of the monoclinic and/or orthorhombic distortion appearance as well as the coexistence of phases. The open question remains the transition detected by thermal expansion above the maximum of dielectric permittivity. Since the thermal expansion is very

sensitive technique to detect any structural modification these “very high” temperature phase transitions can be attributed to the disappearance of the polar nanoregions (PNR). As it is obviously known the polar nanoregions appears at the so called Burns temperature [26, 27] and X-ray diffraction as well as the dielectric measurements do not detect their presence. The symmetry is considered as the cubic one ( $Pm\bar{3}m$ ), however according to the local scale measurements the presence of the polar nanoregions embedded in the nonpolar cubic matrix was evidenced [28-31].

The sequence of phase transitions observed in poled and unpoled PMN-29%PT single crystal and PMN-34.5%PT textured ceramic can be well summarized in Table 1. The thermal expansion and dielectric results clearly show that the poling conditions change and enhance the phase transition sequences for the solid solution with the certain PT content. This is especially well seen in the case of PMN-29%PT composition, see as example the differences between the thermal expansion curves recorded for the FC poled single crystals: FC 20°C (i.e. field cooled from 250°C up to 20°C ) and FC 40°C (i.e. field cooled from 250°C up to 40°C ) presented in Figure 5. The careful analysis of this Figure suggests that both curves can be decomposed into two characteristic sequences. The first sequence, appearing in the bump form, starts near  $\sim 20^\circ\text{C}$ , has a maximum at  $120^\circ\text{C}$  and vanishes at about  $140^\circ\text{C}$  whereas the second one, more significant, appears at about  $130^\circ\text{C}$ , possesses the maximum near  $150^\circ\text{C}$  and finishes at about  $175^\circ\text{C}$ . The first sequence dominates for the FC 20°C crystal while the second one dominates in the case of FC 40°C. Note that intermediate state is observed in the case of RT polarization. This complex behaviour can point to the presence of rhombohedral and monoclinic ordering at room temperature which development is strongly dependent on the kind of polarization. During FC 20°C the sample is cooled till the temperature when the monoclinic symmetry appears while in the case of FC 40°C

the polarization procedure is stopped in the vicinity of the structural phase transition (see Table 1). This suggests that the repeated polarisation/depolarisation cycles might be used as a method of material education. Further discussion of this problem will be presented in our next article.

### ***Raman signature of the PMN-PT***

The perovskite structure (general formula  $ABO_3$ ) is made of two sublattices, a covalent-bonded lattice formed of  $BO_6$  octahedra sharing their oxygen atoms and an A-cation sublattice for which Coulombian interactions are important. For the PMN-PT materials the sublattice A is occupied by  $Pb^{2+}$  ions while the B site by (more or less?) randomly distributed  $Mg^{2+}$ ,  $Nb^{5+}$  and  $Ti^{4+}$  ions (see the hypothetical scheme of the B-cation distribution in Figure 6). From the vibrational point of view, the Raman signature of covalent-bonded structure can be described as that of the covalent entities constituting the structure ( $BO_6$  octahedron). The other ions are highly ionic and contribute with the translation oscillation modes ( $T'$ ) (low energy, below  $\sim 250\text{ cm}^{-1}$ ) which couple themselves with other vibrational modes of the neighbouring entities: translations ( $T'$ ) and rotations/librations ( $R'$ ) of ionic-covalent  $BO_6$  entity leading to the wavenumber shifts. Low wavenumber region ( $100 - 250\text{ cm}^{-1}$ ) chiefly involves cationic network and the lattice modes while a  $250$  to  $800\text{ cm}^{-1}$  spectral range reveals the bending and stretching modes of the covalent-bonded octahedron [3,33].

Figure 7 compares the Raman spectra recorded for FC poled/ unpoled PMN-29%PT single crystal and RT poled/ unpoled PMN-34.5%PT textured ceramic. It was not possible to record the low wavenumber bands below  $70\text{ cm}^{-1}$  in the case of PMN-29%PT. The difficulties are due to the small size of crystal in combination with complicated domain structure and/or polarization effects. The Raman spectra presented

in Figure 7 are typical for relaxor ferroelectrics [3,17,18,33-37]. They consist of a number of broad bands observed in the whole measured temperature range, even within the paraelectric cubic phase with the  $Pm3m$  space group. Note that for such cubic symmetry the first order Raman activity is not allowed [38,39]. This phenomenon has already been connected with the short range intrinsic disorder and the presence of the polar nanoregions (PNR) where the ions are displaced from their high mean symmetry positions giving rise to the local electric dipoles [3,17,18,35-37,40]. Since the Raman spectroscopy is sensitive to the atomic dynamics (through the wavenumbers) and the local electric charge transfer (through the intensities), the local electric defects strongly disturb the spectra, especially intensities [41]. It must be stressed that the origin of the observed Raman spectra is not clear. They can originate from the particular local structure/regions or the coexistence of different phases ordered for a different scale [17,35,42]. According to the previous attempts of mode assignment [33,37] as well as by the comparison with the Raman signatures of the lead oxide perovskites [32] the low frequency region can be attributed to the  $[Pb^{2+}]-[BO_6]$  T' and stretching /lattice modes; the modes from the intermediate frequency region can be classified as mixed B-O-B bending modes while those from the high frequency region as  $BO_6$  stretching vibrations [3,6]. Note that in the B site there are three different ions: Nb, Mg and Ti (see Figure 6). In general, the Raman spectra of a compound made of domain with different composition will not reflect the signature of all regions. Since the Raman cross section depends mainly on the bond polarisability, i. e. the number of electron involved in the bond, the following values of the Raman mode intensities are expected: Nb-O > Ti-O > Mg-O. In consequence, the contribution of Mg-rich regions are too weak to be observed as far as the bending and stretching modes are considered.

### ***Temperature evolution of Raman spectra***

As it can be seen in Figure 7, at a first view, the observed Raman spectra of PMN-29%PT single crystal, both FC poled and unpoled, do not vary very much with the temperature. The Raman spectra of the RT poled and unpoled textured ceramics are also similar except the low wavenumber part (Figure 8). For the unpoled PMN-34.5%PT the mode located near  $50\text{ cm}^{-1}$  is well seen in the whole measured temperature range whereas in the case of RT poled sample this mode significantly softens/disappears in the vicinity of  $140^\circ\text{C}$ . Note that at this temperature the phase transition to the cubic paraelectric phase is detected by the dielectric measurements (see Figure 2).

The quantitative changes of the Raman spectra of both compounds versus temperature were determined in the decomposition process based on the model with minimal number of modes presented in our earlier paper [3,6]. Figure 9 presents as example the decomposed Raman spectra for poled PMN-34.5%PT ceramic in a several values of temperature. Note that the spectra shown in Figure 9 as well as all decomposed spectra were corrected by the Bose-Einstein population factor.

### ***Temperature evolution of the wavenumbers***

The temperature dependences of the wavenumbers for some selected Raman modes characteristic for poled and unpoled: PMN-29%PT and PMN-34.5%PT are presented in Figure 10. Note that dashed lines represent the phase transitions temperature determined from the dielectric and thermal expansion measurements (Figure 2). Additionally, Table 2 contains the wavenumbers of all observed modes for both materials at room temperature, at the temperature of main phase transition to the paraelectric state and at  $240^\circ\text{C}$ . The temperature evolutions of wavenumbers are very similar for PMN-29%PT and PMN-34.5%PT. As it can be clearly seen the

wavenumbers of modes located near  $800\text{ cm}^{-1}$  ( $\text{NbO}_6$  stretching vibrations) do not vary much with the temperature increasing. In contrary, the wavenumbers of modes present near  $570\text{ cm}^{-1}$  ( $\text{TiO}_6$  stretching vibrations as main contribution) exhibit strong temperature sensitivity. Namely, for these modes the wavenumber decreasing of about  $40\text{ cm}^{-1}$  is observed with the anomalous increases of the wavenumber values above the maximum of dielectric permittivity ( $\sim 170^\circ\text{C}$ ). Note that this maximum at  $170^\circ\text{C}$  corresponds well to the additional phase transition recorded during the thermal expansion measurements. Similar behaviour, i.e. significant wavenumber increase with the highest value not at the highest temperature but near  $170^\circ\text{C}$  appears in the case of the  $280\text{ cm}^{-1}$  mode (Ti-O). The temperature dependences of the wavenumbers show thus that the  $\text{NbO}_6$  octahedra are stable during temperature increasing while  $\text{TiO}_6$  ones softens continuously. This shows that the wavenumbers of the modes assigned as Ti-O as well as Nb-O exhibit the anomalous, non-classical temperature evolution. In general, in the “classical case” a wavenumber value decreases with the temperature increasing due to the thermal expansion effects. These anomalous phenomena observed for PMN-PT materials can be related to the expansion/contracting, well seen by the thermal expansion curves (Figure 2, 3), due to the rearrangement of the local structure. During the expansion the maximal value of the dielectric constant is achieved while the decrease of dielectric permittivity is associated with the strong contracting.

For the poled and unpoled PMN-34.5%PT solid solutions we can analyse also the temperature evolution of the wavenumber of the mode present near  $50\text{ cm}^{-1}$  (Figure 8) assigned as the Pb ion sublattice vibrations. The wavenumbers of these modes decrease with temperature increasing, achieving the minimal values near the phase transition temperatures. This evidences the presence of the “step transitions” of the  $\text{Pb}^{2+}$  ion sublattice (Figure 10). The phenomena are again more clear for RT poled ceramic.

### *Temperature evolution of the FWHMs and intensities*

The temperature dependences of the full width at half maxima (FWHMs) and intensities are very similar for poled and unpoled: PMN-29%PT and PMN-34.5%PT solid solutions. Therefore, Figure 11 shows as example these dependences for the poled and unpoled PMN-34.5%PT ceramic. As it can be clearly seen in Figures 7, 8 and 9 the widths of the Raman lines recorded at room temperature for both PMN-PT materials are very characteristic. Namely, the internal modes observed in the middle and high frequency range are rather broad ( $\sim 60 \text{ cm}^{-1}$ ) whereas the widths of external modes measured in the low wavenumbers are rather thin ( $\sim 20 \text{ cm}^{-1}$ ) in comparison with those from the higher frequency range as usually observed for many perovskites [43,44]. The presence of broad bands is typical for disorder materials. In the case of PMN-PT the disorder is especially well observed for modes attributed to the O-B-O bending and B-O stretching vibrations because of the presence in the B-site different elements (see Figure 6) with different ionic-covalent character (covalent Nb, ionic Mg).

With the temperature increasing the significant width increases are observed in the case of lines from the middle and high wavenumber ranges. This is especially well seen in the case of modes located near  $270 \text{ cm}^{-1}$  (Ti-O bending mixed and R' modes) and  $570 \text{ cm}^{-1}$  (Ti-O stretching modes) since their widths increase enormously (Figure 11). The abrupt increase of the line widths appears for both modes in the vicinity of the low temperature phase transition, i.e.  $60^\circ\text{C}$ . Since this transition is not well marked by the dielectric measurements this can suggest that the observed structural modification originates from the significant change of the local structure without the formation of a strong dipole. Above  $60^\circ\text{C}$  the continuous increasing of the FWHMs is observed. Such behaviour points to the high level of structural disorder which strongly affects the both

stretching and bending vibrations of the  $\text{TiO}_6$  octahedra. The FWHMs of the modes located near  $800\text{ cm}^{-1}$  also increase with the temperature, however the increase is rather small what confirms the stability of the  $\text{NbO}_6$  octahedra. In contrary, the FWHMs of modes located near  $50\text{ cm}^{-1}$  ( $\text{Pb}^{2+}$  vibrations) do not change very much with the temperature. Surprisingly, the highest values of the FWHM are not observed at the highest temperature but close to the temperature characteristic for structural phase transitions. This is well seen for the RT polarized sample. Similar FWHM behaviour was already detected for the PMN-PT solid solutions [17,36] and attributed to the Pb ion off-centred displacements: disordered or correlated for the short range scale (nanodomains). This points to the important role of the Pb ion sublattice in the physical behaviour of the PMN-PT system. It should be stressed that the significant differences between the temperature behaviour of the FWHMs of the lattice modes and those ones attributed to the  $\text{BO}_6$  vibrations are characteristic for the perovskite materials and confirm our description in terms of two independent sublattices. [32,43,44].

As it can be seen in Figure 11 the intensities of all modes decrease significantly with the temperature increasing. According to the X-ray diffraction the high temperature symmetry is cubic with the  $\text{Pm}3\text{m}$  space group [9-18]. As we already mentioned for such symmetry the first order Raman activity is forbidden. The presence of the Raman modes reveals that the symmetry at least in the local, Raman scale is lower than this cubic one. Therefore, the significant intensity decreases suggest that with the temperature increasing the local symmetry evolves continuously towards the cubic one. These results fit well with the last phase transition observed on thermal expansion curve (Figure 2), close to  $200^\circ\text{C}$  and thus show that the true cubic symmetry can be achieved only at rather high temperature, i.e. much above the maximum of dielectric permittivity.

However, one of the recent article [44] suggests that the nanoclusters with lower symmetry are present in pure PMN up to  $\sim 550^{\circ}\text{C}$ .

Finally, it should be underlined that the values of FWHMs, intensities as well as the wavenumbers show the maximal or minimal values near the phase transitions temperatures determined from the dielectric and thermal expansion measurements (dashed lines). It is possible small discrepancies between the values of phase transition temperatures obtained from different experiments. Note that characteristic extremes determined from the Raman spectra correspond especially well to the phase transition temperatures detected in the thermal expansion measurements. This shows huge sensibility of both techniques to detect modifications of the chemical bonds.

#### ***Temperature evolution of Rayleigh wings***

Parallel to the Raman spectra at each value of temperature the Raman spectra in the both sides of the Rayleigh line were recorded with a lower resolution (Rayleigh wings). Since the Rayleigh intensity is direct proportional to the dielectric and compositional heterogeneity this allowed studying the subtle temperature modification what was especially valuable for PMN-29%PT for which the low wavenumber region of the Raman spectrum was cut. It is noteworthy that in the case of relaxors in vicinity of the Rayleigh line the central peak can be observed because of the lattice relaxations [35,46]. Additionally, in the low wavenumber range another interesting phenomenon is expected, namely the presence of the soft modes. Inelastic neutron scattering studies [47,48] point to the existence of the ferroelectric soft mode in PMN which becomes overdamped near the temperature in which the polar nanoregions appear, i.e. Burns temperature [26]. However, the similar behaviour has not been confirmed by the Raman studies. It must be stressed, that the investigation of the soft mode and central peak are

not the subject of this article and we do not try to separate the different contributions: Rayleigh broadening, central mode, overdamped mode, etc .

The analysis of the Rayleigh wings allowed us to determine the temperature dependences of the intensities and widths. However, it should be noted that these values were not obtained due to the decomposition/fitting but using the so called triangle method: the Rayleigh peak intensities are normalised and the low wavenumber scattering (Rayleigh wings) is approximated by a triangle. Figure 12 compares the temperature dependences of the Rayleigh wings intensities and widths with the thermal expansion and dielectric results. The dashed lines mark the phase transition temperatures determined from the dielectric and thermal expansion results. Note that near very similar values of temperature the significant step variation of intensity and a maximum of the widths are observed. Such important changes of intensity, especially well seen for poled samples, can be associated with the rearrangement of the ferroelectric domain state which directly influence the optical properties of the material. This shows that the Rayleigh wing intensity that probes the compositional and dielectric heterogeneity appears as sensitive to the nanostructure rearrangement as the temperature dependences of the of Raman wavenumbers.

## Conclusion

PMN-29%PT single crystal and PMN-34.5%PT textured ceramic were investigated in a wide temperature range by the thermal expansion, dielectric and Raman spectroscopy. These studies show that both materials possess the complex sequence of the phase transitions characteristic to the PMN-PT solid solutions from the vicinity of the MPB. It is noteworthy that new phase transitions were evidenced at 40°C, 91°C and 180°C in the case of FC PMN-29%PT as well as at 70°C and 200°C for

RT PMN-34.5%PT. The physical behaviours of the PMN-29%PT single crystal and PMN-34.5%PT textured ceramic are very similar. Any differences seem to be rather connected with the different compositions/ B heterogeneity distribution as well as the kind of the poling condition (FC or RT) than to the form (single crystal, textured ceramic). This is very important from the application point of view. It could be assumed that material education could modify the phase equilibrium as well as sequence and hence maximize the dielectric properties, as made for some materials with martensitic phase transition. This deserves further studies. The thermal expansion data show the strong expansion which allow to the rearrangements of the local structure. During such expansion the maximal values of the dielectric permittivity are achieved. In consequence the disappearance of the ferroelectric properties is associated with the presence of the strong volume changes (and hence stress in anisotropic ceramic which can in return modify the phase transition sequence). The presence of the thermal hysteresis, well seen in the thermal expansion and dielectric measurements, suggests that the most of observed phase transition have the first order character.

The presence of the Raman spectra within the cubic paraelectric phase reveals that the symmetry at least at the local, Raman scale, i.e. a nanoscale, is lower than the cubic one ( $Pm3m$ ). However, the significant decrease of the Raman line intensities with the temperature increasing shows that the symmetry evolves continuously towards the cubic one.

The temperature dependences of the Raman wavenumbers and FWHMs suggest the existence of the Nb-rich and Ti-rich nanoregions (see sketch in Figure 6). The wavenumbers and FWHMs of the modes attributed to the  $NbO_6$  vibrations are almost independent on the temperature changes what reveals the high stability of the  $NbO_6$  octahedra. In contrary the  $TiO_6$  octahedra are very sensitive: with the temperature

increasing the wavenumbers soften continuously and the significant increases of the FWHMs are observed. The most drastic increases of the FWHMs appear in the vicinity of the low temperature phase transitions. These results point to the Ti-O bond elongation and the formation of the dipole in the  $\text{TiO}_6$  clusters leading to the strong disorder. Note that our studies do not bring any information about  $\text{MgO}_6$  octahedra ( $\text{Mg-O}$  bonds exhibit very poor Raman scattering). However, the strong ionic character of the  $\text{Mg}^{2+}$  allowed to suggest the existence of the coupling of the  $\text{MgO}_6$  modes with those ones characteristic to the  $\text{TiO}_6$  and  $\text{Pb}^{2+}$  vibrations. Raman studies evidenced also the step transitions of the  $\text{Pb}^{2+}$  ion sublattice. The highest FWHM values of these mode are also observed near the phase transition temperatures. This shows that the  $\text{TiO}_6$  and  $\text{Pb}^{2+}$  sublattices are especially affected. In consequence, the structural phase transitions as well as the dielectric properties are the effect of the strong coupling between these affected sublattices. It should be stressed that the homogeneity of the Ti ions distribution plays also the key role in the electromechanical properties of the PLZT optoelectronic ceramics [49,50]. The presence of the phase transitions determined from the dielectric and thermal expansion data is rather well confirmed by the temperature dependences of the intensity and width of the Rayleigh wings. This shows that the Rayleigh wings appear very sensitive to the nanostructure rearrangement. It should be stressed that the further careful analysis of low frequency range is important because it can clarify the presence/overdamping of the soft mode in the PMN-PT system. Finally, our results reveal that the temperatures and character of the phase transitions are different for poled FC/unpoled PMN-29%PT single crystal as well as RT poled/unpoled PMN-34.5%PT textured ceramic. This confirms that the kind of the polarization plays the key role on the local structure and hence electromechanical properties of PMN-PT system. The pooling cycles appears to be a method for the optimisation of the

ferro/piezoelectric properties. It must be stressed that the similar study performed in the RT poled single crystal and FC poled textured ceramic will be the subject of our next article.

Accepted manuscript

## References

1. S.-E. Park and T.R. Shrout, *J. Appl. Phys.* **82** (1997)1804
2. H. Fu and R. H. Cohen, *Nature* **403** (2000)281
3. M. Pham Thi, G March and Ph Colomban *J. Eur. Ceram. Soc.* **25** (2005) 3335
4. M. Pham Thi, Ph. Colomban and O. Lacour \*Proc. 50th UFFC, 2004 IEEE International Ultrasonics, Ferroelectrics and Frequency Control Joint 50th Anniversary Conference, 23-27 Août 2004, Montréal\*
5. M. Pham Thi, Proc. Materiaux 2006 N°1362, 13-17 Novembre 2006, Dijon, France
6. A. Slodczyk, M. Barre, F. Romain, Ph. Colomban, M. Pham-Thi, *J. Phys: Conference Series* **92** (2007) doi:10.1088/1742-6596/92/1/012159
7. E. M. Sabolsky, A. R. James, S. Kwon, S. Trollier-McKinstry and G. L. Messing: *Appl. Phys. Lett.* **78** (2001) 2551.
8. E. M. Sabolsky, S. Trollier-McKinstry and G. L. Messing: *J. Appl. Phys.* **93** (2003) 4072
9. W. Choi, T.R. Shrout, S. J. Jang and A.S. Bhalla, *Ferroelectrics* **100** (1989) 29
10. O. Noblanc, P. Gaucher and G. Calvarin, *J. Appl. Phys.* **79** (1996) 4291
11. B. Noheda, D. E. Cox, G. Shirane, J. Gao and Z.-G. Ye: *Phys. Rev. B* **66** (2002) 054104.
12. A. K. Singh and D. Pandey, *J. Phys.: Condens. Matter* **13** (2001) L931
13. A. Kumar Singh and D. Pandey: *Phys. Rev. B.* **67** (2003) 064102.
14. G. Xu, H. Luo, H. Xu and Z. Yin, *Phys. Rev. B* **64** (2001) 020102
15. D. Zekria, V. A. Shuvaeva and A. M. Glazer, *J. Phys.: Condens. Matter* **17** (2005) 1593

16. V. A. Shuvaeva, A. M. Glazer and D. Zekria, *J. Phys.: Condens. Matter* **17** (2005) 5709
17. A. Slodczyk, Ph. Daniel and A. Kania, *Phase Transitions* **79** (2006) 399
18. Ph. Colomban and M. Pham Thi *Mater. Res. Soc. Symp. Proc.* **855E** (2005) W3.1.1
19. D. Vanderbilt and M. H. Cohen, *Phys. Rev. B* **63** (2001) 094108
20. J Kreisler, B Dkhil, P Bouvier and J Kiat *Phys.Rev B* **65** (2002) 172101
21. F Bai, N Wang, J Li, D Viehland, P Gehring, G Xu and G Shirane *J. Appl. Phys.* **96** (2004) 1620
22. Z. G. Ye, B. Noheda, M. Dong, D. Cox and G. Shirane *Phys. Rev B* **64** (2001) 184114
23. L. E. Cross, *Ferroelectrics* **76** (1987) 241
24. G. A. Samara, *J. Phys.: Condens. Matter* **15** (2003) R367
25. R. R. Chien, V. H. Schmidt and Ch. S. Tu, *J. Cryst. Growth* **287** (2006) 454
26. G. Burns and F. H. Dacol, *Phys. Rev. B* **28** (1983) 2527
27. K. Hirota, Z. G. Ye, S. Wakimoto, P. M. Gehring and G. Shirane, *Phys. Rev. B* **65** (2002) 104105
28. C. A. Randall, A. S. Bhalla, T. R. ShROUT and L. E. Cross, *J. Mater. Res.* **5** (1990) 829
29. Y. Yan, S. J. Pennycook, Z. Xu and D. Viehland, *Appl. Phys. Lett.* **72** (1998) 3145
30. E. Prouzet, E. Husson, N. de Mathan and A. Morell, *J. Phys.: Condens. Matter* **5** (1993) 4889
31. R. Blinc, A. Gregorovic, B. Zalar, R. Pirc, V. V. Laguta and M. D. Glinchuk, *Phys. Rev. B* **63** (2000) 024104

32. Ph. Colomban, F. Romain, A. Neiman and I. Animitsa , *Solid State Ionics* **145** (2001) 339-347
33. E. Husson, L. Abello and A. Morell, *Mater. Res. Bull.* **25** (1990) 539
34. H. Ohwa, M. Iwata, H. Orihara, N. Yasuda and Y. Ishibashi, *J. Phys. Soc. Jap.* **70** (2001) 3149
35. O. Svitelskiy, J. Toulouse, G. Yong and Z. G. Ye, *Phys. Rev. B* **68** (2003) 104107
36. A. Slodczyk, A. Kania, Ph. Daniel, A. Ratuszna, *J. Phys. D: Appl. Phys.* **38** (2005) 2910
37. S. A. Prosandeev, E. Cockayne, P. B. Burton, S. Kamba, J. Petzelt, Yu. Yuzyuk, R. S. Katiyar and S. B. Vakhrushev, *Phys. Rev. B* **70** (2004) 134110
38. A. E. Pasto, R. A. Condrate, (1973) The laser Raman spectra of several perovskite zirconates, *Adv. Spectrosc. Vol 1*, J.P. Mathieu Ed., Heyden & Sons Ltd, London,
39. R. A. Frey (1973) The crystal structure of  $\text{PbTiO}_3$ , *Adv. Spectrosc. Vol 1*, J.P. Mathieu Ed, Heyden & Sons Ltd, London,
40. M. Iwata, H. Hoshino, H. Orihara, H. Ohwa, N. Yasuda and Y. Ishibashi *Japan. J. Appl. Phys.* **39** (2000) 5691
41. Ph. Colomban and G. Lucazeau *J. Chem. Phys.* **72** (1980) 1213
42. R. Haumont, P. Gemeiner, B. Dkhil, J. M. Kiat and A. Bulou, *Phys. Rev. B* **73** (2006) 104106
43. G. Gouadec and Ph. Colomban *Prog. Cryst. Growth Charact. Mater.* **53** (2007) 1
44. I. Animitsa, T. Denisova, A. Nieman, A. Nepryahin, N. Kochetova, N. Zhuraviev, Ph. Colomban *Solid State Ionics* **162-163** (2003) 73

45. R. Kesavamoothy and V. Sivasubramanian, *J. Raman Spectrosc.* **38** (2007) 762
46. J. Toulouse, F. Jiang, O. Svitelskiy, W. Chen, and Z. G. Ye, *Phys. Rev. B* **72** (2005) 184106
47. P. M. Gehring, S. Wakimoto, Z. G. Ye, and G. Shirane, *Phys. Rev. Lett.* **87** (2001) 277601
48. S. Wakimoto, C. Stock, R. J. Birgeneau, Z. G. Ye, W. Chen, W. J. L. Buyers, P. M. Gehring, and G. Shirane, *Phys. Rev. B* **65** (2002) 172105
49. Ph. Colomban, *Ceramics International* **15** (1989) 23
50. Ph. Colomban (2005) *Chemical Processing of Ceramics*, Second Edition, S. Komarnemi and B. Lee Eds, CRC Press Boca Raton, FL, USA

Accepted manuscript

**Figure captions**

**Figure 1.** Scheme of the PMN-PT phase diagram according to the data of Choi et al [9], Noblanc et al [10] and Noheda et al [11] Letters: C, R, T and M denote the cubic, rhombohedral, tetragonal and monoclinic symmetry. The morphotropic phase boundary region is dashed

**Figure 2.** Temperature dependences of the thermal expansion and dielectric permittivity for FC poled/unpoled PMN-29%PT single crystal (SC) and RT poled/unpoled PMN-34.5%PT textured ceramic (TC). The arrows marked the heating and cooling cycles

**Figure 3.** Thermal expansion curves recorded along x, y, z orthogonal directions of the cut ceramic close to the [100], [010] and [001] crystallographic directions showing the anisotropic character of the PMN-34.5%PT textured ceramic

**Figure 4.** Temperature hysteresis revealed in the temperature dependences of the dielectric permittivity for FC poled PMN-29%PT single crystal and RT poled PMN-34.5% textured ceramic

**Figure 5.** Thermal expansion curves recorded for FC poled 20°C (i.e. field cooled from 170°C up to 20°C), RT poled and FC poled 40°C (i.e. field cooled from 170°C up to 40°C) PMN-29%PT single crystals. Note that the FC pooling conditions can significantly change the properties of the material while RT polarization leads to the intermediate state.

**Figure 6.** Hypothetical scheme of the A-cation and B-cation ( $\text{NbO}_6$ ,  $\text{MgO}_6$  and  $\text{TiO}_6$  octahedra) distribution in the PMN-PT lattice. The Nb-rich (rectangles) and Ti-rich (circles) nanoregions are marked

**Figure 7.** Raman spectra recorded for FC poled/ unpoled PMN-29%PT single crystal and RT poled/ unpoled PMN-34.5%PT textured ceramic

**Figure 8** Low wavenumber regions of the Raman spectra with clear differences between the RT poled and unpoled PMN-34.5%PT textured ceramic

**Figure 9.** Decomposed Raman spectra for poled PMN-34.5%PT ceramic in a several values of temperature. For a clear comparison the spectra have been corrected by the Bose-Einstein population factor.

**Figure 10** Temperature dependences of the wavenumbers for some selected Raman modes characteristic for poled and unpoled PMN-29%PT and PMN-34.5%PT. The dashed lines mark the characteristic temperatures of the phase transitions determined from the dielectric and thermal expansion results

**Figure 11.** Temperature dependences of the full width at half maxima (FWHMs) and intensities for RT poled and unpoled PMN-34.5%PT textured ceramic. The dashed lines mark the characteristic temperatures of the phase transitions determined from the dielectric and thermal expansion results

**Figure 12** Temperature dependences of the Rayleigh wings intensities and widths compared with the thermal expansion and dielectric results. The dashed lines mark the characteristic temperatures of the phase transitions determined from the dielectric and thermal expansion results

Accepted manuscript

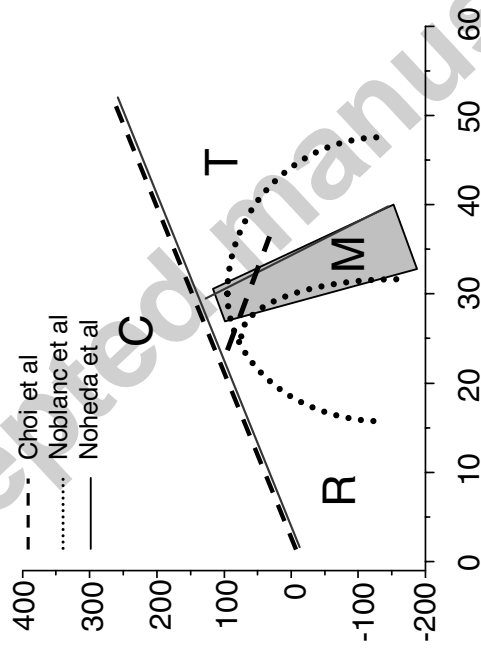
**Table 1** The sequence of phase transitions observed in poled and unpoled PMN-29%PT single crystal and PMN-34.5%PT textured ceramic. The letters: C, R, T, M1, M2 denote the cubic, rhombohedral, tetragonal, monoclinic (Pm), monoclinic (Cm) symmetry, respectively while PNR means the polar nanoregions.

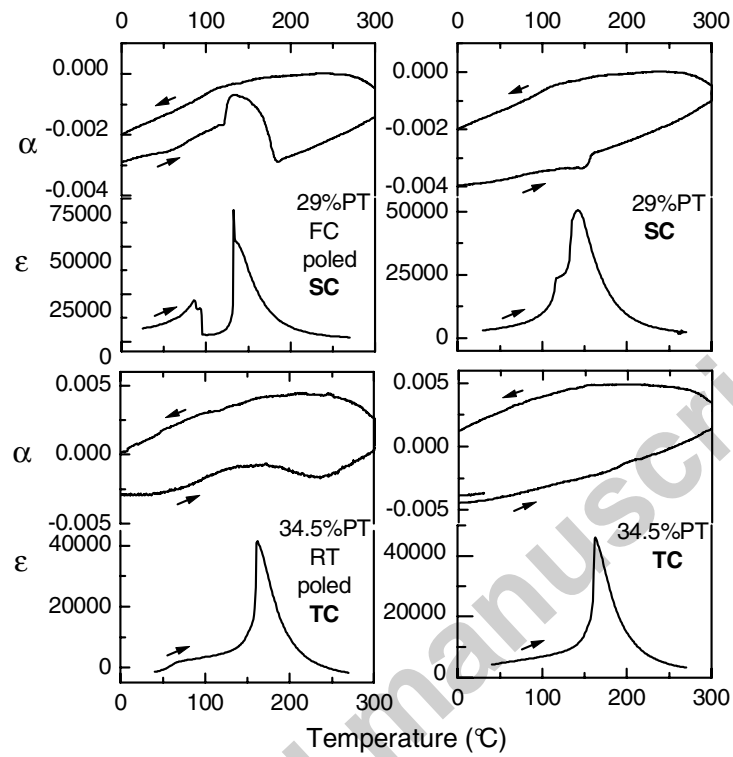
<b>FC poled PMN-29%PT single crystal</b>					
Temperature (°C)	40		91	134	180
Phase transition features	M1? M2? (ferro)	M1/M2?; M+R?, M1+M2 ? (ferro)	R (ferro)	C	C without PNR ?
<b>unpoled PMN-29%PT single crystal</b>					
Temperature (°C)			118	140	
Phase transition features	M1?, M+R? (relaxor)		R (relaxor)	C	
<b>RT poled PMN-34.5%PT textured ceramic</b>					
Temperature (°C)	70		160		200
Phase transition features	M1? M2? (ferro)	T (ferro)		C	C without PNR ?
<b>unpoled PMN-34.5%PT textured ceramic</b>					
Temperature (°C)			160		
Phase transition features	T (ferro)			C	

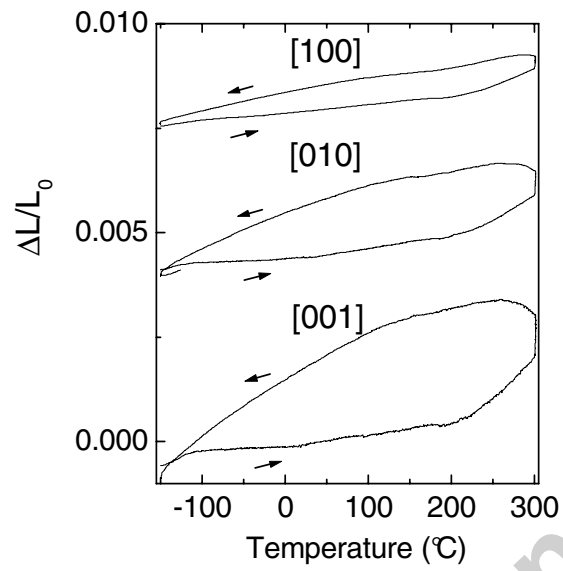
**Table 2** (part a and b) Wavenumbers of all observed modes of poled (FC/RT) and unpoled: PMN-29%PT and PMN-34.5%PT at a few characteristic temperatures: RT, temperature of the main phase transition to the paraelectric state ( $\sim 140^\circ\text{C}$  for PMN-29%PT and  $\sim 160^\circ\text{C}$  for PMN-34.5%PT) and  $240^\circ\text{C}$ , the temperature of the "cubic" state). The assignment of modes is also proposed (note that the mode couplings are neglected).

Samples & Polarization	[Pb <sup>2+</sup> ]-[BO <sub>6</sub> ], T <sup>a</sup> vibrations/lattice modes (cm <sup>-1</sup> )						TiO <sub>6</sub> bending (cm <sup>-1</sup> )						NbO <sub>6</sub> bending (cm <sup>-1</sup> )									
	RT	PT	240°C	RT	PT	240°C	RT	PT	240°C	RT	PT	240°C	RT	PT	240°C	RT	PT	240°C	RT	PT	240°C	
FC PMN- 29%PT	-	-	-	-	-	-	-	-	-	222	-	-	268	267	270	321	-	-	-	-	443	-
Unpoled PMN- 29%PT	-	-	-	-	-	-	-	-	-	223	-	-	263	265	266	324	-	-	-	-	443	-
RT PMN- 34.5%PT	56.8	55.1	54.8	68.2	-	-	132	122	120	220	-	-	275	285	283	325	-	-	-	-	446	-
unpoled PMN-34 .5%PT	57.2	55.7	55.2	69.4	-	-	138	124	122	219	-	-	280	283	282	327	-	-	-	-	446	-

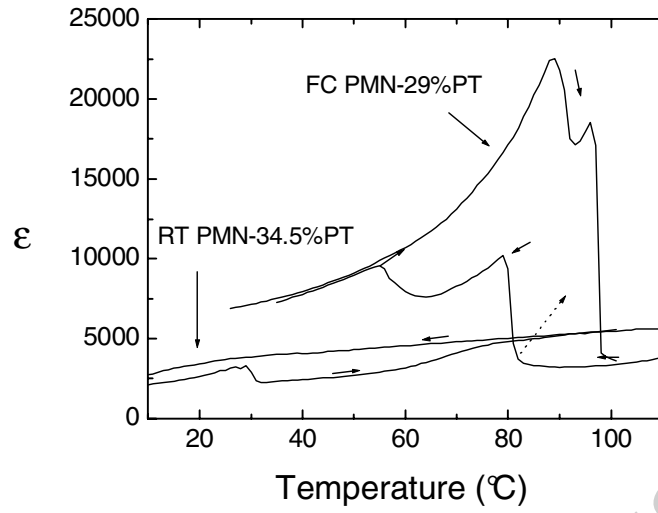
Samples & Polarization	TiO <sub>6</sub> stretching						NbO <sub>6</sub> stretching					
	RT	PT	240°C	RT	PT	240°C	RT	PT	240°C	RT	PT	240°C
FC PMN- 29%PT	517	-	-	577	560	508	748	764	756	793	799	801
Unpoled PMN- 29%PT	515	-	-	581	561	522	763	760	760	799	802	797
RT PMN- 34.5%PT	522	-	-	575	545	513	740	740	744	797	799	798
unpoled PMN-34 .5%PT	522	-	-	581	558	538	743	741	740	798	799	800

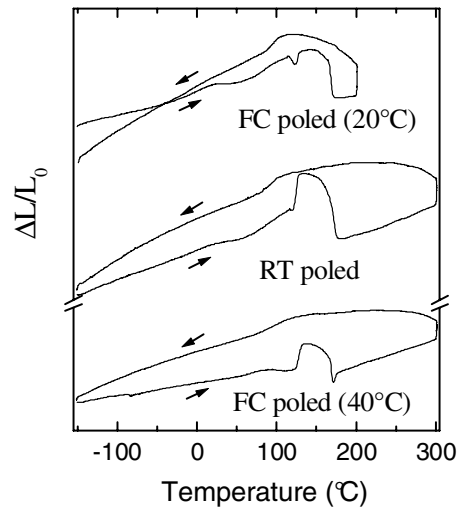




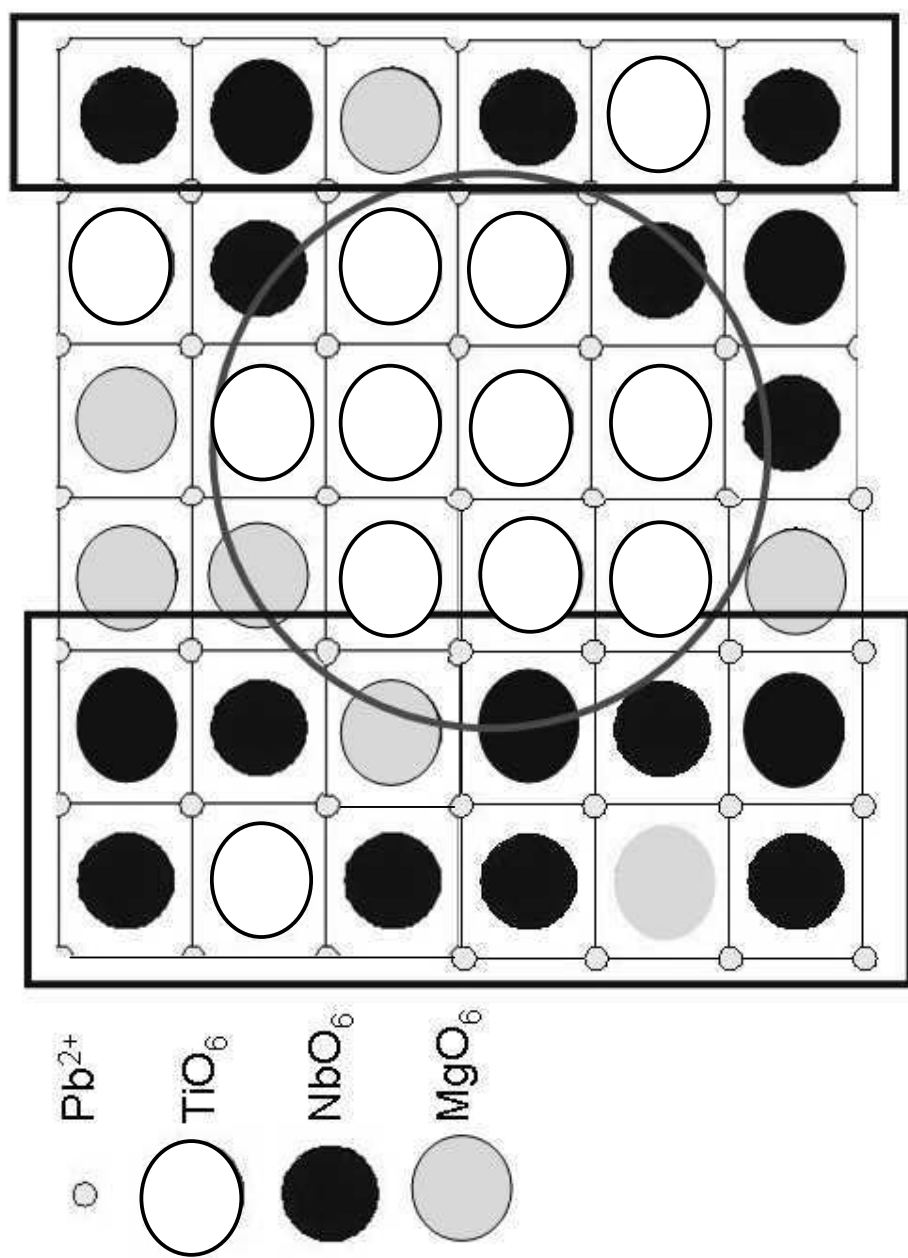


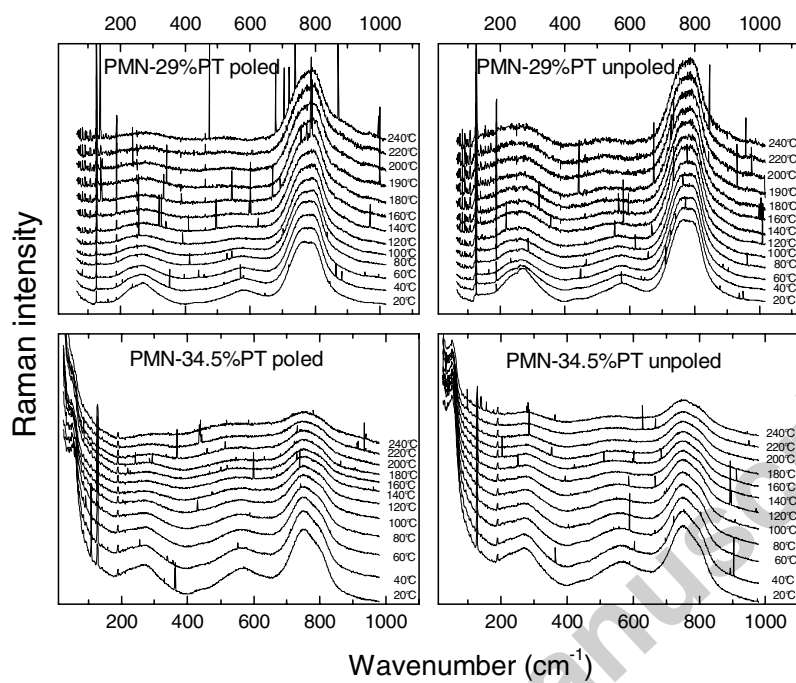
Accepted manuscript

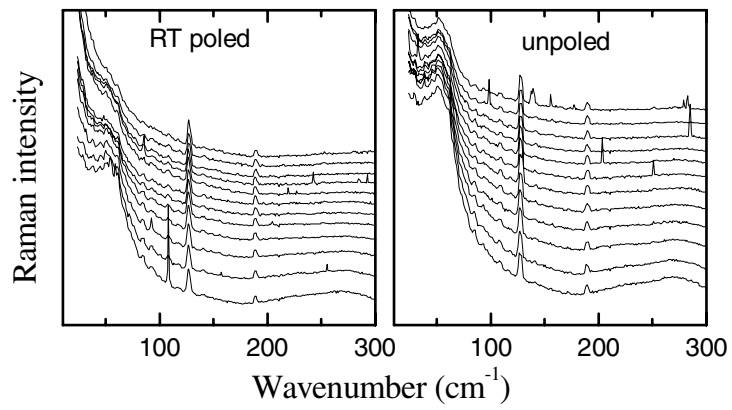




Accepted manuscript







Accepted manuscript

